Insight of the glacier dynamics in the region of Qaanaaq, Greenland, using infrasound data

Sentia Oger[1], Patrick Hupe[2]
[1]CEA DAM DIF, F-91297, Arpajon, France
[2]BGR (Federal Institute for Geosciences and Natural Resources), Hannover, Germany

Context

The sea level rise is increasing with a current rate of 3.7 mm/y over the period 1900 – 2020 compared to a rate of 1.7 mm/y over the period 1900 – 2020 [IPCC AR6], with a current contribution of the Greenland by 26 % and more to come. However multiple challenges remain, as understanding the processes behind the Greenland ice mass loss, which is necessary for its prediction, through climate modeling. Within the Comprehensive nuclear-Test-Ban Treaty Organization, infrasound stations were set up worldwide. One is located at Qaanaaq, in Greenland. It gathers a total of 17 years of measurements, which represents a high potential for timeseries analyses, in view to study the evolution of the local cryosphere. While it was suggested to possibly record glaciers-related processes [Evers et al., 2022], no study deeply investigated this record.

Can we fill the knowledge gap on the variability of local Greenland ice mass, especially around the Qaanaaq region, from the annual to the subseasonal scales ?
Can we document the processes related to this ice loss ?

Current sea level rise and projections from the two IPCC pathways RCP2.6 and 8.5

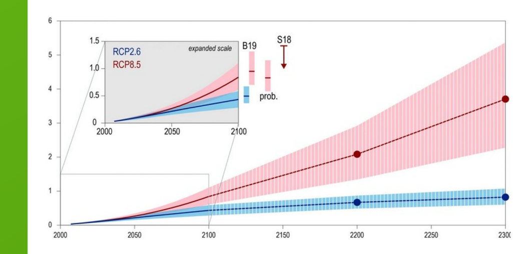

Adapted from Oppenheimer, IPCC SROCC, 2019

Main contributions to sea level rise

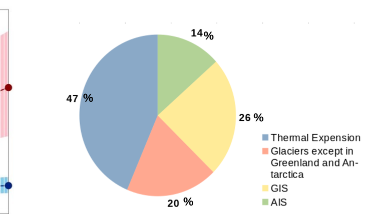

Greenland mass change

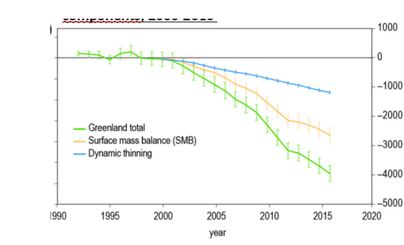

II Methodology

II.a Extraction of a multivariate dataset

The I18DK infrasound data from the International Monitoring System

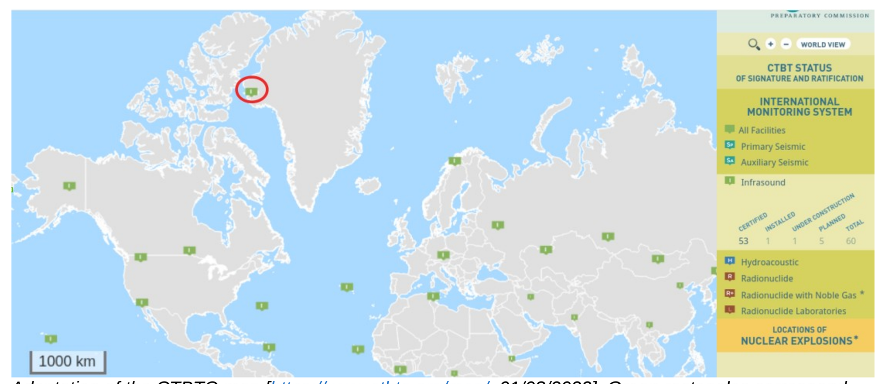

Adaptation of the CTBTO map [https://www.ctbto.org/map/, 01/08/2022]. Green rectangles correspond the location of the infrasound stations. The red circles point the I18DK station.

Installation of the I18DK station [https://www.ctbto.org/verification-regime/featured-stations/ types/infrasound/is18-qaanaaq-greenland-denmark/, 01/08/2022].

ID CARD

Location : **77.45°N, 290.71°E**

- Initiated in the CTBT context
- Maintained by the **Danish Meteorological Institute**
- Data sent to the IMS laboratory in Vienna

Eight-element infrasonic array divided into two sub-arrays equipped with wind noise reduction systems and a Central Processing Facility

Data covering the period **04/2004-12/2020**

Post-processing : PMCC [Cansi et al., 1995]

Outputs : Mean frequency, back-Azimuth, Celerity and Amplitude

PREPROCESSING

Each sensor measures an overpressure (in Pa).

The Progressive Multi-Channel Correlation (PMCC) is applied on the set of signals to extract the wave front parameters of the coherent plane waves :

- **Mean Frequency (Hz)**
- **Back-azimuth (°)**
- **Celerity (m/s)**
- **Amplitude (Pa)**

Data are then **filtered** :
- Consistency > 0.05
- 320 m/s < Celerity < 360 m/s
- Mean Frequency > 1 Hz

Finally, **dayly means** are processed.

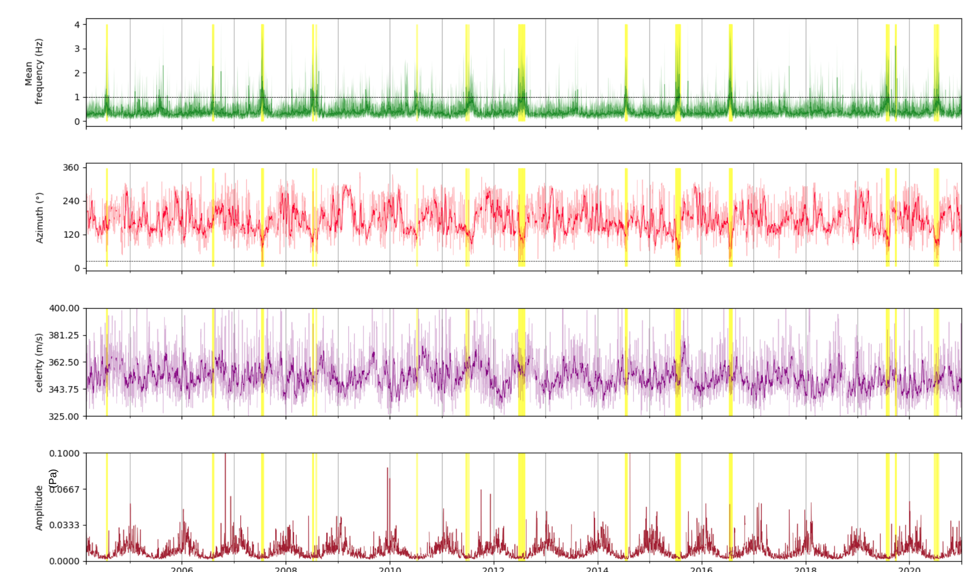

Daily means of the I18DK wave front parameters over the period 2004-2020 : The Mean Frequency (green line, in Hz), the back-azimuth (red line, in Hz), the celerity (purple line, in m/s), and the amplitude (brown, in Pa). Yellow vertical lines highlight frequencies higher than 3 Hz.

KEY POINTS 1 :
- **Seasonal cycles** appear highlighting **a strong climate forcing** at the seasonal scale.
- Events with frequencies higher than 2 Hz are recorded.
- These « **high-frequency** » **events** appear every year during the summer at the exception of years 2009, 2013, 2017 and 2018.
- They are associated with relative low back azimuths, high celerities and low amplitudes.

Climate outputs

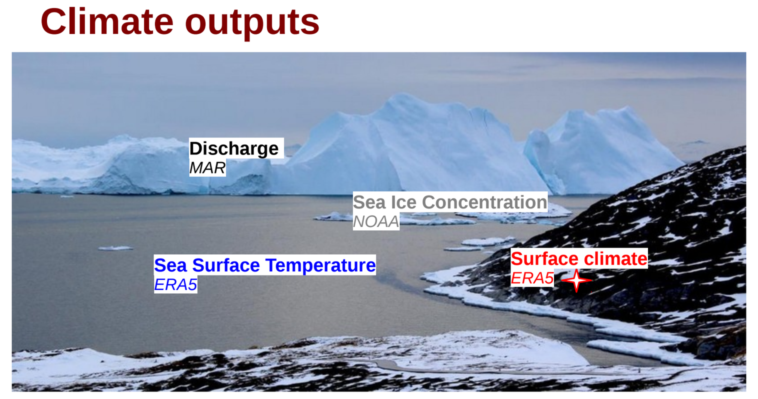

Scheme Photography by Michalea King. https://oceanographicmagazine.com/news/greenland-glaciers-ice-loss/, 01/08/2022.

The ERA5 reanalyses :
- **[Local] 2m-Temperature**
- **[Local] 10m-u and v wind components**
- **[Regional] Sea-Surface Temperature**

Time resolution : month averages from daily outputs

Grid resolution : 30 km

Coordinate of the grid point :

Covered period : 2004 – 2020

2m-Temperature, u and v wind components extracted for the grid point corresponding to Qaanaaq

Sea Surface Temperature averaged over the grid points Of the bay (see image on the right)

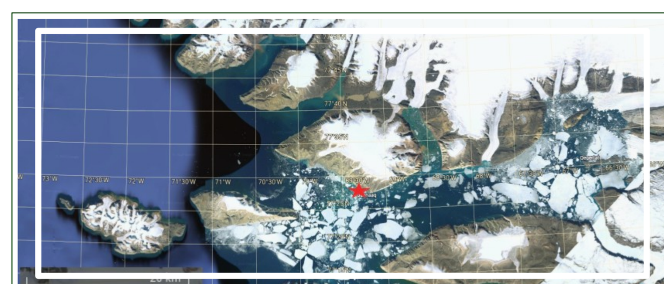

Region surrounding Qaanaaq (red star). The withe rectangle correspond to the area selected to extract mean sea surface temperature and ice concentration. Google Map image, 01/08/2022.

National Snow & Ice Data Center

[Regional] Sea Ice Concentration
Satellite product

Time resolution : day

Grid resolution : 4 km

Region : lat=[77°-78°] ; lon=[-73°-65°]

Covered period : 2013-2020

Greenland liquid water discharge simulated by Region Climate Models

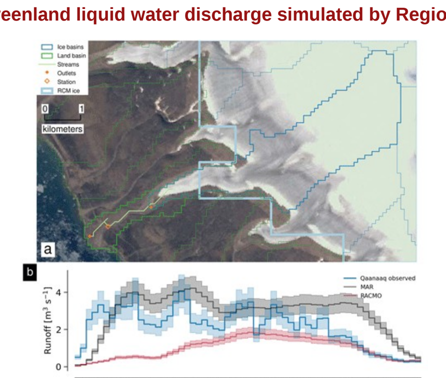

Discharge outputs. Adapted from Mankoff et al., Earth Syst. Sci. Data, 2020. (a) reprensents a satellite image of the area arount Qaanaaq, (b) annual discharge time series.

Liquid water discharge
Simulations of discharge from

- Ice basins
- Land basins
- Streams
- Outlets

By the Regional Climate Models **MAR and RACMO.**

MAR slightly overestimates the discharge, with absolute difference with the data lower than the RACMO model and thus was preferentially used.

Covered period : 2013-2019

Daily scale

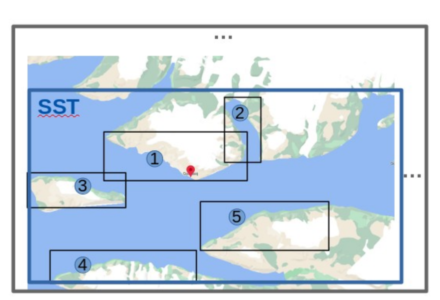

Selected regions of averaged discharges. The red point corresponds to Qaanaaq. The five regions are annotated by black rectangles. The blue rectangle show again the area selected to average the sea surface temperature (SST) output simulated by ERA5.

Five regions were extracted :

(1) Around Qaanaaq, lat=[77.45 ; 77.70] ° lon=[-70.20 ; -68.53] °

(2) Bowdoin Glacier, lat=[77.45 ; 77.56] ° lon=[-68.90 ; -68.40] °

(3) Island, lat=[77.38 ; 77.48] ° lon=[-71.30 ; -70.77] °

(4) Far opposite coastline, lat=[72.25 ; 77.17] ° lon=[-70.90,-69.10] °

(5) Near opposite coastline, lat=[77.27 ; 77.41] ° lon=[-69.1 ; -67.4] °

II.b Timeseries analysis

- **Preliminaray analyses : Timeseries, Distributions / Histograms, Pearson correlations**
- **Climate variability : seasonal to annual scales, tendencies**
- **Machine learning algorithms based on interpretability – Random Forest**

III Results

Preliminary analyses

Distribution of the number of detections in function of the 1°-averaged back-azimuths and by seasons

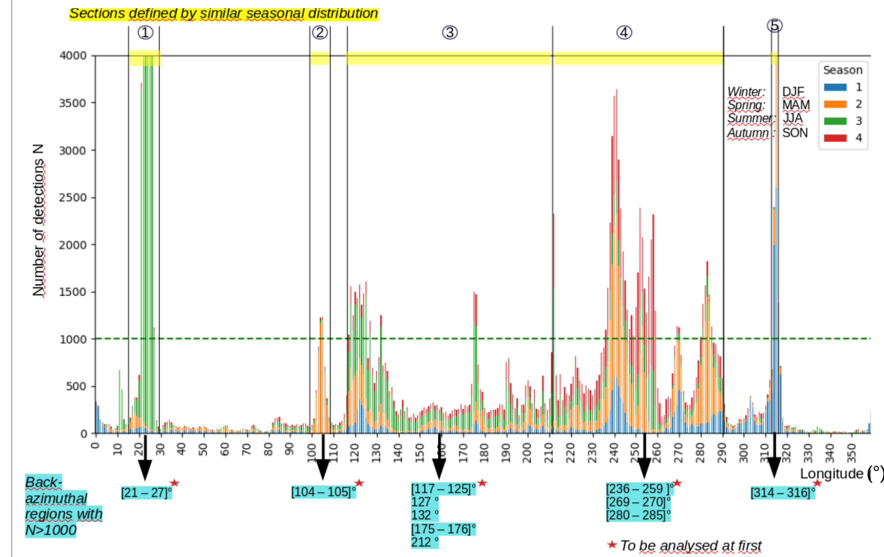

Description of the different sections : Back-azimuth, season and potential cause

1. **Section 1**
   - The highest number of detections
   - Summer signal
   - Point toward the Qaanaaq glacier
2. **Section 2**
   - Relatively narrow back-azimuth range value
   - Autumn signal
   - Point toward the inner bay and the opposite coastline
   - Could record sea ice or glacier-related processes
3. **Section 3**
   - Point the main opposite coastline
   - Mixed seasons signal, mainly autumn and summer
   - Could record sea ice or glacier-related processes

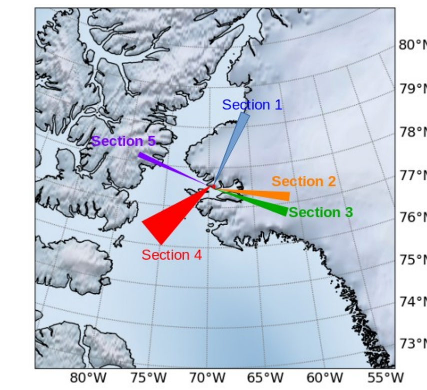

Sections of back-azimuths 1 – 5.

4. **Section 4**
   Point the main opposite coastline
   Mixed seasons signal, mainly autumn and spring
   Could record sea ice or glacier-related processes
5. **Section 5**
   Very narrow back-azimuth range value
   Winter signal
   Toward Baffin bay

Seasonal distribution of the the different sections

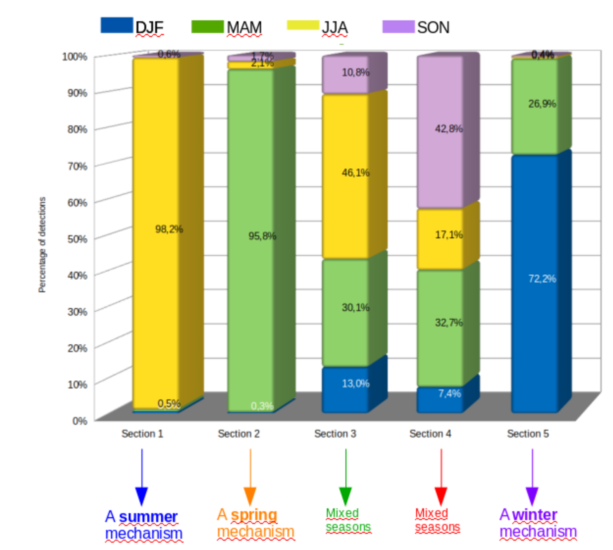

KEY POINTS 2 :
- We choose a **threshold for the total number of detections, of 1000** to consider a 1°-averaged back azimuth.
- The detections display **different seasonal distributions.**
- **5 sections** of back-azimuths can be distinguished by their seasonal distributional.

Climate variability

Seasonal distribution of the different sections at the daily scale

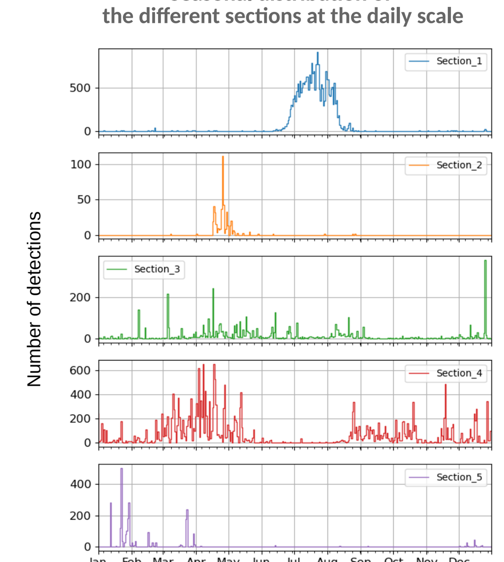

Seasonal distribution of the climate variables

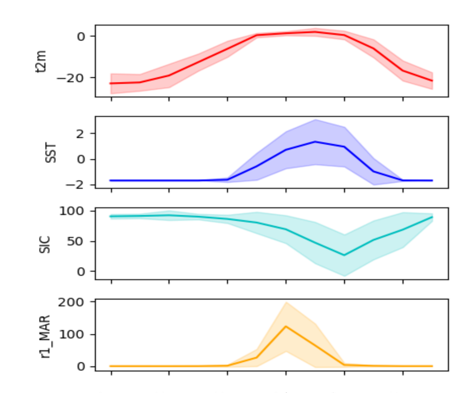

KEY POINT 3
- Except for the section 1, the seasonal distribution of the number of detections by sections make appear **no clear seasonal cycles.**
- At the seasonal scale, the comparison with the climate variables is not straightforward.

Annual variability of the number of detections in the different sections and trends at the annual scale

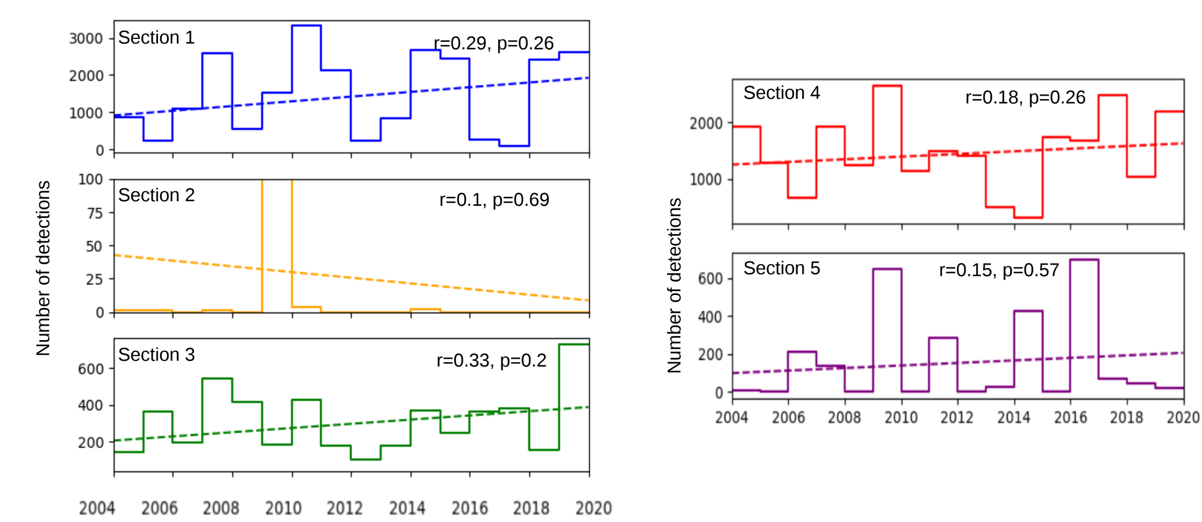

KEY POINT 4
- The high number of detections associated with **section 2 are condensed in 2009** and thus, might be due to a strong event this year. This section is **discarded** in the following.
- **No significant trend** for any section : consistent with Greenland sea ice concentration and elevation change trends reported in the literature.

Machine learning to help in the interpretability

Illustration of the Random Forest

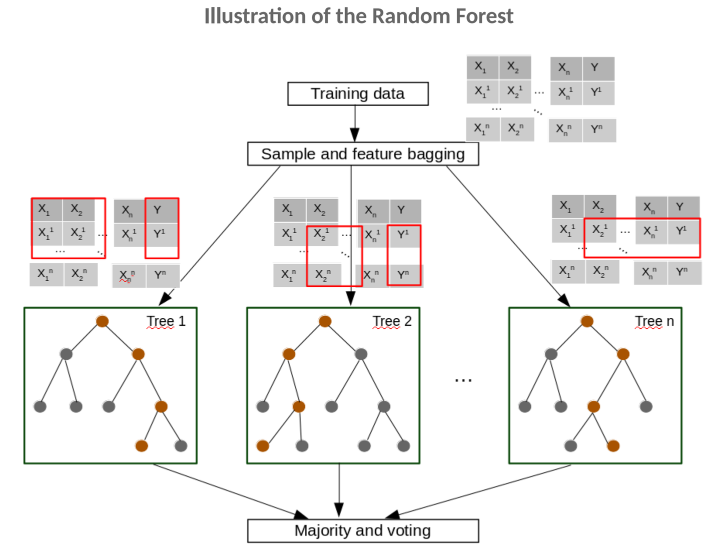

Machine learning can be used to **associate causes to effects** : this is the interpretability.

Beyond the possible machines, the **Random Forest** consist of a set of decision trees, **allowing the representation of features importance.**

Here, for each section, we train random forests to predict an infrasound detection, given the aforementioned climate variables (surface air temperature, sea surface temperature, wind components, sea ice concentration and water discharges).

Results are acceptable for the section 1.

Prediction of the detections from section 1

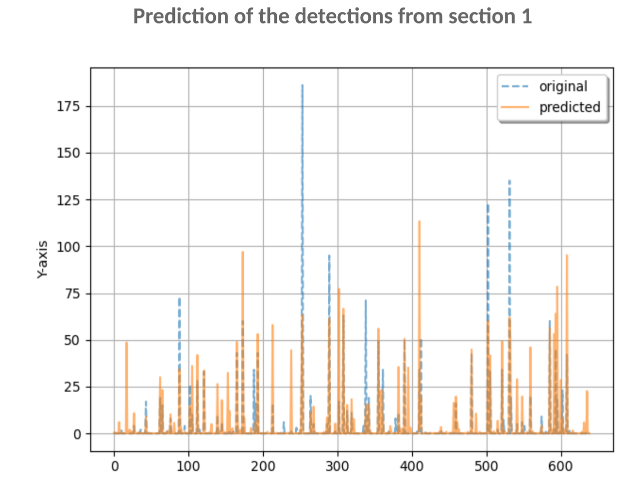

Feature importance from the predictions of the detections from section 1

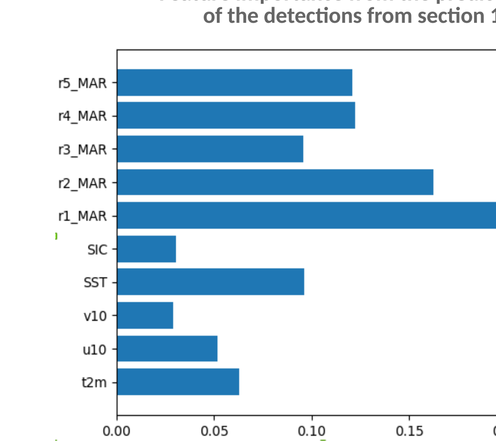

KEY POINT 5
- The regression of the number of detections in section 1 is acceptable (MSE and RMSE).
- The feature importance is in favor of processes related to the Qaanaaq glacier and its discharge.

IV Conclusions and perspectives

A first machine learning baseline based on a Random forest regressor, was built in order to predict infrasound detections coming from the Qaanaaq Glacier. The features importance indicates a main contribution from water discharge in this area, compared to climate variables such as the local surface air temperature, the regional sea surface temperature and sea ice concentrations. A finer description of the features, as well as other machines will be explored in the future.

References

Oppenheimer, M., Glavovic, B., Hinkel, J., Van de Wal, R., Magnan, A. K., Abd-Elgawad, A., ... & Sebesvari, Z. (2019). Sea level rise and implications for low-lying islands, coasts and communities, IPCC Special Report on the Ocean and Cryosphere in a Changing Climate, edited by: Pörtner, H.-O., Roberts, DC. See https://www. ipcc. ch/srocc/chapter.
Evers, L. G., Smets, P. S. M., Assink, J. D., Shani-Kadmiel, S., Kondo, K., & Sugiyama, S. (2022). Long-Term Infrasonic Monitoring of Land and Marine-Terminating Glaciers in Greenland. Geophysical Research Letters, 49(8), e2021GL097113.
Rignot, E., & Mouginot, J. (2012). Ice flow in Greenland for the international polar year 2008–2009. Geophysical Research Letters, 39(11).
Mouginot, J., Rignot, E., Bjørk, A. A., Van den Broeke, M., Millan, R., Morlighem, M., ... & Wood, M. (2019). Forty-six years of Greenland Ice Sheet mass balance from 1972 to 2018. Proceedings of the national academy of sciences, 116(19), 9239-9244.
Cansi, Y. (1995). An automatic seismic event processing for detection and location: The PMCC method. Geophysical research letters, 22(9), 1021-1024.
Hersbach, H., Bell, B., Berrisford, P., Hirahara, S., Horányi, A., Muñoz-Sabater, J., ... & Thépaut, J. N. (2020). The ERA5 global reanalysis. Quarterly Journal of the Royal Meteorological Society, 146(730), 1999-2049.
Evers, L. G., Smets, P. S. M., Assink, J. D., Shani-Kadmiel, S., Kondo, K., & Sugiyama, S. (2022). Long-Term Infrasonic Monitoring of Land and Marine-Terminating Glaciers in Greenland. Geophysical Research Letters, 49(8), e2021GL097113.
Fetterer, F., J. S. Stewart, and W. N. Meier. 2015, updated daily. MASAM2: Daily 4 km Arctic Sea Ice Concentration, Version 1. [indicate subset used]. Boulder, Colorado USA. NSIDC: National Snow and Ice Data Center.
Mankoff, K. D., Noël, B., Fettweis, X., Ahlstrøm, A. P., Colgan, W., Kondo, K., ... & Fausto, R. S. (2020). Greenland liquid water discharge from 1958 through 2019. Earth System Science Data, 12(4), 2811-2841.

Aknowledgements

We thank Alexis Le Pichon for having facilitated the exchanges and its pieces of advices for the post treatment data.